Polymorphic energy ordering of MgO, ZnO, GaN, and MnO within the random phase approximation

Haowei Peng* and Stephan Lany†
National Renewable Energy Laboratory, Golden, Colorado 80401, USA
(Received 1 April 2013; published 30 May 2013)

Accurate relative energetic stabilities between the tetrahedrally coordinated (zinc-blende or wurtzite) and octahedrally coordinated (rock-salt) phases of MgO, ZnO, GaN, and MnO are obtained by first-principles calculations within the framework of adiabatic connection fluctuation-dissipation theorem (ACFDT) and with the random phase approximation (RPA) to the correlation energy. The RPA-ACFDT correctly recovers the rock-salt structure of MnO as the ground-state phase, as observed experimentally, whereas previous density and hybrid functional methods obtained the wrong energy ordering. Even though standard density functionals give the correct ordering of the non-transition-metal compounds, significant quantitative changes occur also for MgO and ZnO. We conclude that the RPA can serve as an important benchmark for structural preferences in polymorphic materials. The present study suggests that density functional predictions for open d-shell materials such as transition metal compounds might be more prone to erroneous structure prediction than commonly expected.

DOI: 10.1103/PhysRevB.87.174113 PACS number(s): 71.15.Nc, 64.60.My, 71.10.−w, 61.50.Ah

I. INTRODUCTION

As a prototypical d^5 transition-metal oxide, MnO has received interest due to potential applications such as magnetic piezoelectric semiconductors,[1] p-type oxides,[2] and photoelectrochemical water-splitting materials.[3,4] The ground-state structure for MnO is rock salt (RS), but very recently metastable wurtzite (WZ) MnO was grown on a carbon template.[5] Schrön *et al.*[6] have studied in detail the relative stability of these two and the zinc-blende (ZB) polymorphs of MnO in various different magnetic configurations, using the generalized gradient approximation (GGA) to density functional theory (DFT), on-site correlations within GGA + U,[7] and the Heyd-Scuseria-Ernzerhof hybrid functional (HSE03).[8] Unless a large and arguably unphysical U parameter is used,[3] the WZ and ZB phases are lower in energy than the experimental observed RS ground state. This finding raises the question of how reliable DFT is in various approximations for structure prediction, especially for transition metal compounds.

Beyond DFT, the total energy can be alternatively obtained within the framework of the adiabatic connection fluctuation-dissipation theorem (ACFDT),[9] which provides a post-DFT approach that calculates the total energy by combining the exact exchange energy (E_{EXX}) and the correlation energy from the random phase approximation (RPA),

$$E_{\mathrm{tot}}^{\mathrm{RPA}} = E_{\mathrm{EXX}} + E_c^{\mathrm{RPA}}. \quad (1)$$

The calculations of the RPA total energy rely on the Kohn-Sham orbitals and eigenvalues from a preceding DFT calculation. Compatible with the RPA total energy, electronic structure properties such as the quasiparticle energies band structure and the density of states can be calculated with the GW method in the RPA.[10] The RPA total energies have been recently assessed for various bulk materials, and they have been found to give a better prediction for lattice constants and bulk modulus, and an equally good or better prediction for atomization energies.[11–13] Hence, it is interesting to study polymorphism based on RPA total energies, in particular for cases such as MnO where DFT methods experience difficulties.

Besides the interest from a methodological point of view, there are also urgent practical demands. The structure-property relation in MnO has been investigated in our previous theoretical study,[2] where we found that the different coordination environment of Mn in the RS and ZB or WZ structures profoundly affects the properties. For example, the fundamental band gap of ZB MnO was predicted to be 2.1 eV, more than 1 eV smaller and with less of an indirect character than in the RS phase.[2] With regard to the electrical properties, the tetrahedral coordination of Mn in the ZB structure was found to suppress the self-trapping of holes, thereby suggesting much better hole-transport properties than in the RS phase, which is a small polaron conductor.[2,14] Thus, stabilizing the tetrahedrally coordinated ZB or WZ phases could lead to new solar energy materials with desirable semiconducting properties, e.g., for photoelectrochemical water-splitting. One approach to stabilize tetrahedrally coordinated Mn is alloying MnO with other compounds favoring the ZB or WZ structure, such as ZnO and GaN. However, since the relative stabilities of the different structures of MnO are not quantitatively known, it remains unclear whether such an approach would be feasible.

For this work, we performed RPA total energy calculations for RS and ZB MnO with antiferromagnetic ordering along the [111] (AF2) and [001] (AF1) directions, respectively, which have been identified as the lowest energy configurations.[6] Since WZ MnO has a larger unit cell (16 atoms in the respective AF1 configuration) than ZB MnO (see Ref. 6 and below), but is almost degenerate in energy, we are considering here the ZB structure as representative of the tetrahedral coordination environment. As a benchmark, and also to facilitate studies on related alloy systems,[3,15–24] we performed RPA-ACFDT calculations for ZnO and GaN in the RS, WZ, and ZB structures, and for MgO in the RS and ZB structures (WZ MgO is not stable[25,26]), where the simple DFT can correctly predict the energy ordering.

 ©2013 American Physical Society

II. COMPUTATIONAL METHODS

All calculations were performed using the VASP code[27,28] and projector augmented wave (PAW) pseudopotentials[29,30] which accurately describe the scattering properties to energy as high as 10 Ry.[9,31] To save computational cost, we choose the soft PAW pseudopotentials for N and O, which enables us to use a relatively low energy cutoff. For the exchange correlation, we employ the GGA with the Perdew-Burke-Ernzerhof (PBE) functional.[32] We first perform PBE calculations for MgO, ZnO, GaN, and PBE + U (Ref. 7) calculations with $U = 3$ eV on Mn d orbitals for MnO, which describes the valence band quite well.[3,33,34] Based on the resulting Kohn-Sham orbitals and eigenvalues, we obtain the RPA-ACFDT results for MgO, GaN, and MnO. However, the RPA-ACFDT calculation for ZnO is based on PBE + U with $U = 6$ eV on Zn d orbitals, which was found in Ref. 35 to provide a better starting point for subsequent GW calculations. For MnO, we further considered calculations with a nonlocal external potential[36] (V) together with the on-site Hubbard U, which are chosen to produce the correct p-d coupling between both occupied and unoccupied Mn d and O p states. We refer to this approach as PBE + V_{GW} in the following, since the GW results are used as a reference during fitting these two parameters (see below for details). The detailed procedure of the RPA-ACFDT calculations follows that described in Ref. 9. The energy cutoffs of the plane-wave basis are 540 eV for MgO and GaN, and 450 eV for ZnO and MnO. The energy cutoffs for the response function are 360 eV for MgO and GaN, and 300 eV for ZnO and MnO. To obtain a well-converged RPA total energy, we use a large number of bands close to the full size of the Hamiltonian matrix, i.e., 640/f.u. for ZB or WZ MgO and GaN, 512/f.u. for RS MgO and GaN, 512/f.u. for ZB or WZ ZnO and MnO, and 400/f.u. for RS ZnO and MnO. For the integration over the Brillouin zone, the $6 \times 6 \times 6$ and $6 \times 6 \times 4$ Monkhorst-Pack[37] k-meshes were employed for the two-atom RS or ZB unit cells and the four-atom RS MnO cell, and the four-atom WZ unit cells and four-atom ZB MnO, respectively. The bulk properties including the relaxed volume, bulk modulus, and total energy for both PBE + U and RPA-ACFDT results are obtained by fitting the Murnaghan equation of state to the calculated total energy (E) and volume (Ω) data sets:

$$E(\Omega) = E_0 + \frac{B_0\Omega}{B_0'}\left(\frac{(\Omega_0/\Omega)^{B_0'}}{B_0' - 1} + 1\right) - \frac{B_0\Omega_0}{B_0' - 1}. \quad (2)$$

Here E_0 and Ω_0 are the equilibrium total energy and volume, and B_0 and B_0' are the bulk modulus at zero pressure and the pressure derivative of the bulk modulus, which is assumed to be a constant.[38] For ZnO and GaN, we further calculated the phase transition pressure P_{tr} at which the Gibbs free energies, here reducing to the enthalpy at zero temperature, of the WZ and RS phases equate to each other.[39] The enthalpy could be expressed as a function of pressure as follows:

$$H(P) = E_0 + \frac{B_0\Omega_0}{B_0' - 1}\left[\left(1 + \frac{B_0'}{B_0}P\right)^{(B_0'-1)/B_0'} - 1\right]. \quad (3)$$

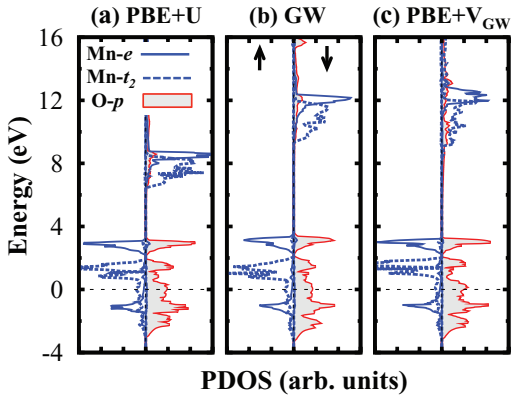

FIG. 1. (Color online) The calculated Mn-d partial density of states (PDOS) in rock-salt (RS) MnO for both spin-up and -down channels. The energy zero is set to the center of mass of the occupied O p PDOS. The e-like Mn d, t_2-like Mn d, and O p states are plotted with solid curves, dashed curves, and shadowed areas, respectively.

III. RESULTS AND DISCUSSION

First, we calculate the total energies of ZB MnO and WZ MnO with the low-energy AF1 and AF3 antiferromagnetic configurations relative to the energy of RS MnO with the AF2 magnetic configuration. The naming of the magnetic configurations is the same as that in Ref. 6 (also see Fig. 1 therein). Both PBE + U with $U = 3$ eV on Mn d orbitals and an HSE06 (Ref. 40) hybrid functional are used, and the results are shown in Table I. As observed before in Ref. 6, the RS structure of MnO is predicted to have a higher energy than the WZ and ZB MnO structures, and the AF1 and AF3 configurations are close in energy for both WZ and ZB MnO. The lowest energy configurations of WZ and ZB lie within 6 meV per formula unit for both PBE + U and HSE06 (see Table I). Hence, the RPA-ACFDT energy of ZB MnO, which can be calculated in a smaller unit cell, should also serve as a good estimate for the WZ structure. In the following, for MnO, "RS" refers to the RS structure with the AF2 magnetic configuration and "ZB" refers to ZB MnO with AF1.

Table II gives the calculated lattice volume (Ω), the total energy per formula unit relative to the experimental ground-state structure (ΔE), and the bulk modulus (B_0), as well as experimental data[41–47] for (Ω) and (B_0) where available. Focusing first on the main group compounds MgO, GaN, and ZnO, we observe that PBE correctly predicts the ground-state structures, and RPA-ACFDT finds the same energy ordering, as expected. However, the relative stability of ZB or WZ with respect to RS polymorphs in MgO and ZnO is significantly

TABLE I. Calculated total energies (meV per formula unit) of WZ and ZB MnO in the AF1 and AF3 magnetic configurations, relative to the energy of RS MnO in the AF2 magnetic configuration.

Structure	RS-AF2	WZ-AF1	WZ-AF3	ZB-AF1	ZB-AF3
PBE + U	0	−22	−19	−19	−18
HSE06	0	−35	−32	−28	−29

TABLE II. The calculated volume (Ω), total energy per formula unit referenced by the experimental ground-state structure (ΔE), and bulk modulus (B_0) for MgO, ZnO, GaN, and MnO, compared with experimental data[41–47] where available.

		PBE-DFT			RPA-ACFDT			Experiment	
Compound	Structure	Ω (AA^3)	B_0 (GPa)	ΔE (meV)	Ω (AA^3)	B_0 (GPa)	ΔE (meV)	Ω (AA^3)	B_0 (GPa)
MgO	RS	19.35	149	**0**	18.87	172	**0**	18.73	160, 165
	ZB	24.70	114	214	24.10	128	297		
ZnO[a]	RS	20.32	164	304	19.90	183	239		202.5
	WZ	24.69	128	**0**	24.26	156	**0**	23.80	183, 143
	ZB	24.67	128	15	24.21	157	20		
GaN	RS	19.44	209	964	19.02	239	976		
	WZ	23.49	171	**0**	23.03	210	**0**	22.81	195, 210
	ZB	23.49	171	13	23.08	207	15		
MnO[b]	RS	22.26	145	**0**	22.57	158	**0**	21.76, 21.83	144–160
	ZB	27.01	108	−19	27.38	114	67		
MnO[c]	RS	24.21	138	**0**	23.04	153	**0**	21.76, 21.83	144–160
	ZB	29.94	103	64	28.35	109	131		

[a]In the RPA-ACFDT calculations, PBE + U with $U = 6$ eV for Zn-d was used to generate the DFT orbitals and eigenenergies.
[b]PBE + U ($U = 3$ eV for Mn d).
[c]PBE + V_{GW} ($U = 7$ and $V = 3$ eV for Mn d).

different from the PBE calculations. The energy of the ZB polymorph of MgO increases from 214 to 297 meV per formula unit, and the energy of RS ZnO decreases from 304 to 239 meV. In a $Mg_xZn_{1-x}O$ alloy, the structure changes from WZ or ZB to RS at a certain critical composition x_c. Because of the small bowing of the mixing energy,[18] we can estimate this critical concentration by $x_c = \delta E_{\mathrm{ZnO}}/(\delta E_{\mathrm{ZnO}} - \delta E_{\mathrm{MgO}})$, where $\delta E = \Delta E_{\mathrm{ZB}} - \Delta E_{\mathrm{RS}}$. Using the numbers in Table II, the PBE and RPA-ACFDT calculations give x_c equal to 0.57 and 0.42, respectively. In previous LDA calculations, $x_c =$ 0.34 was obtained.[18] Our present RPA result lies within the range $0.33 < x < 0.45$ for the WZ to RS transition reported by Chen *et al.*,[21,22] but we acknowledge that there are considerable variations between different experimental reports.[19,20,23,24] As shown in Table II, the bulk modulus and unit-cell volume (lattice constants) for these three compounds are also improved by the RPA-ACFDT calculations, in good agreement with the trends discussed in Refs. 11 and 12. The phase-transition pressure P_{tr} for ZnO and GaN from WZ to RS is 12.09 and 45.36 GPa from PBE-DFT, and 9.18 and 42.52 GPa from RPA-ACFDT. The PBE-GGA results here agree well with previous GGA calculations, but are systematically higher than the corresponding LDA results.[39,48] For ZnO, the RPA-ACFDT result agrees better with experimental value of 9.1 GPa,[45] while both the RPA-ACFDT and PBE-GGA results for GaN are well located in the experimental values from 37 to 52.2 GPa.[48]

In the case of the transition metal oxide MnO, the situation is more complicated. Both PBE + U and HSE06 wrongly predict that RS MnO is higher in energy than ZB MnO (see Table I), which contradicts the experimental observation. To study the electronic origin of this failure, we plot in Figs. 1(a) and 1(b) for RS MnO the partial density of states (PDOS) of occupied and unoccupied Mn d states, relative to the "center of mass" of the occupied O p states, calculated in PBE + U and GW, respectively. Note that for ZB MnO, the respective PDOS plots are quite similar, except that the energy ordering of the "e" and "t_2" level is interchanged.[2] Obviously, the exchange splitting is largely underestimated in PBE + U compared to the GW calculations, implying that the p-d hybridization between the O p and unoccupied Mn d^0 orbitals of compatible symmetry (i.e., e and t_2 in RS and ZB, respectively) is overestimated in PBE + U.[49] Since this p-d^0 coupling forms an occupied bonding state and an empty antibonding state,[2] it leads to an energy gain. The magnitude of the energy gain depends on (i) the degeneracy of the bonding or antibonding state (doubly degenerated in RS, and triply in ZB), (ii) the energy difference between the atomic orbitals, (iii) the atomic distance between Mn and its O ligands (2.23 and 2.06 Å in RS and ZB, respectively), and (iv) the overlapping of the wave functions (e directly pointing to the O ligands in RS, but not in ZB[2]). It is difficult to directly estimate the magnitude of energy gain for RS and ZB MnO which is determined by the subtle balance of the factors mentioned above, however, as implied by the lower total energy of ZB in the PBE + U or HSE06 calculations, the tetrahedrally coordinated ZB polymorph appears to benefit more from this spurious effect than the octahedrally coordinated RS structure.

To reduce this overestimated p-d^0 hybridization, we introduce a potential V_{GW} to reproduce the relative energies of both the occupied Mn d^5 and the unoccupied Mn d^0 states with respect to the O p states obtained from GW, thereby correcting the too strong p-d^0 hybridization in the wave functions (Kohn-Sham orbitals). This potential V_{GW} is constructed by an on-site Hubbard U (Ref. 7) in conjunction with a nonlocal external potential V (Ref. 36) on Mn d orbitals. The former separates the occupied Mn d^5 and unoccupied Mn d^0 states in energy, and the latter shifts both together relative to the O p states. (Note that simply increasing the value of U in PBE + U to reproduce the exchange splitting of GW would place the occupied Mn d state too low in energy.) Using the V_{GW} with $U = 7$ eV and $V = 3$ eV, we obtain a PDOS that is very similar to that of the GW calculations for both RS [see Fig. 1(c)] and ZB MnO. Calculating the ZB or RS energy difference directly in PBE + V_{GW}, we obtain the correct energy ordering, but the lattice constant becomes too large with an error of 3.6% compared with experimental

data (Table II). The changed energy ordering in PBE + V_{GW} confirms that the underestimated exchange splitting is the main cause for the wrong structure prediction in PBE + U.

As shown in Table II, using the PBE + U orbitals and eigenvalues as input, the RPA-ACFDT calculations correctly obtain the RS polymorph as the ground state with a lower energy than ZB by 67 meV per formula unit. While the RPA total energy accounts for the change of the quasiparticle energies in a corresponding RPA-GW calculation,[10,31] it is still based on the overly hybridized wave functions of PBE + U. Thus, we performed also RPA-ACFDT calculations based on the PBE + V_{GW} solutions, which further increases the ZB energy by about 60 meV per formula unit. This additional stabilization of the RS structure can be attributed to the change of the p-d^0 wave-function hybridization when the unoccupied Mn d states are lifted up in energy to match the GW prediction. Note that the RPA-ACFDT also largely corrects the lattice constant overestimation in the direct PBE + V_{GW} calculation, and that the bulk modulus in the RPA is in good agreement with experiment irrespective of the underlying DFT Hamiltonian. The resulting preference for MnO in favor of the octahedral RS structure by 131 meV is still less than the respective preference for ZnO in favor of the tetrahedral WZ or ZB structures, indicating that Zn alloying of less than 50% in MnO should induce a transition toward the desirable tetrahedral structure.

IV. CONCLUSIONS

In conclusion, RPA-ACFDT corrects the energy ordering of the MnO polymorphs, which was wrongly predicted in PBE + U and HSE06 calculations due to the underestimated exchange splitting of Mn d states. An additional energy gain of the RS polymorph is obtained when the overestimated p-d^0 hybridization is corrected, indicating that the wave-function character plays a significant role for the RPA-ACFDT energy in open-shell systems such as the d^5 configuration in MnO. This finding implies that in such systems, the prediction of the correct energy ordering of polymorphs could quite generally be sensitive to the accuracy of the orbital energies given by the respective Hamiltonian. For the non-transition-metal compounds, standard DFT is qualitatively correct as expected, but there are non-negligible quantitative changes of the structure preference of MgO and ZnO in RPA-ACFDT.

ACKNOWLEDGMENTS

This work is supported by the US Department of Energy, Office of Science, Office of Basic Energy Sciences, Energy Frontier Research Centers, under Contract No. DE-AC36-08GO28308 to NREL. The high performance computing resources of the National Energy Research Scientific Computing Center and of NREL's Computational Science Center are gratefully acknowledged.

*Haowei.Peng@NREL.gov
†Stephan.Lany@NREL.gov

[1] P. Gopal, N. A. Spaldin, and U. V. Waghmare, Phys. Rev. B **70**, 205104 (2004).
[2] H. Peng and S. Lany, Phys. Rev. B **85**, 201202 (2012).
[3] D. K. Kanan and E. A. Carter, J. Phys. Chem. C **116**, 9876 (2012).
[4] M. C. Toroker and E. A. Carter, J. Mater. Chem. A **1**, 2474 (2013).
[5] K. Nam, Y. Kim, Y. Jo, and S. Lee, J. Am. Chem. Soc. **134**, 8392 (2012).
[6] A. Schrön, C. Rödl, and F. Bechstedt, Phys. Rev. B **82**, 165109 (2010).
[7] S. L. Dudarev, G. A. Botton, S. Y. Savrasov, C. J. Humphreys, and A. P. Sutton, Phys. Rev. B **57**, 1505 (1998).
[8] J. Heyd, G. E. Scuseria, and M. Ernzerhof, J. Chem. Phys. **118**, 8207 (2003).
[9] J. Harl and G. Kresse, Phys. Rev. B **77**, 045136 (2008).
[10] L. Schimka, J. Harl, A. Stroppa, A. Grüneis, M. Marsman, F. Mittendorfer, and G. Kresse, Nat. Mater. **9**, 741 (2010).
[11] J. Harl and G. Kresse, Phys. Rev. Lett. **103**, 056401 (2009).
[12] J. Harl, L. Schimka, and G. Kresse, Phys. Rev. B **81**, 115126 (2010).
[13] J. Yan, J. S. Hummelshøj, and J. K. Nørskov, Phys. Rev. B **87**, 075207 (2013).
[14] A. Bosman and H. van Daal, Adv. Phys. **19**, 1 (1970).
[15] K. Maeda, T. Takata, and M. Hara, J. Am. Chem. Soc. **127**, 8286 (2005).
[16] K. Maeda and K. Domen, Chem. Mater. **22**, 612 (2010).
[17] S. Wang and L.-W. Wang, Phys. Rev. Lett. **104**, 065501 (2010).
[18] Y. Z. Zhu, G. D. Chen, H. Ye, A. Walsh, C. Y. Moon, and S.-H. Wei, Phys. Rev. B **77**, 245209 (2008).
[19] A. Ohtomo, M. Kawasaki, T. Koida, K. Masubuchi, H. Koinuma, Y. Sakurai, Y. Yoshida, T. Yasuda, and Y. Segawa, Appl. Phys. Lett. **72**, 2466 (1998).
[20] T. Minemoto, T. Negami, and S. Nishiwaki, Thin Solid Films **372**, 173 (2000).
[21] J. Chen, W. Shen, N. Chen, D. J. Qiu, and H. Z. Wu, J. Phys.: Condens. Matter **15**, L475 (2003).
[22] N. Chen and C. Sui, Mater. Sci. Eng. B **126**, 16 (2006).
[23] Z. Vashaei, T. Minegishi, H. Suzuki, T. Hanada, M. W. Cho, T. Yao, and A. Setiawan, J. Appl. Phys. **98**, 054911 (2005).
[24] C. Bundesmann, A. Rahm, M. Lorenz, M. Grundmann, and M. Schubert, J. Appl. Phys. **99**, 113504 (2006).
[25] S. Limpijumnong and W. R. L. Lambrecht, Phys. Rev. B **63**, 104103 (2001).
[26] A. Schleife, F. Fuchs, J. Furthmüller, and F. Bechstedt, Phys. Rev. B **73**, 245212 (2006).
[27] G. Kresse and J. Hafner, Phys. Rev. B **47**, 558 (1993).
[28] G. Kresse and J. Hafner, Phys. Rev. B **49**, 14251 (1994).
[29] P. E. Blöchl, Phys. Rev. B **50**, 17953 (1994).
[30] G. Kresse and D. Joubert, Phys. Rev. B **59**, 1758 (1999).
[31] M. Shishkin and G. Kresse, Phys. Rev. B **74**, 035101 (2006).
[32] J. P. Perdew, K. Burke, and M. Ernzerhof, Phys. Rev. Lett. **77**, 3865 (1996).
[33] J. van Elp, R. H. Potze, H. Eskes, R. Berger, and G. A. Sawatzky, Phys. Rev. B **44**, 1530 (1991).
[34] C. Rödl, F. Fuchs, J. Furthmüller, and F. Bechstedt, Phys. Rev. B **77**, 184408 (2008).
[35] L. Y. Lim, S. Lany, Y. J. Chang, E. Rotenberg, A. Zunger, and M. F. Toney, Phys. Rev. B **86**, 235113 (2012).

[36]S. Lany, H. Raebiger, and A. Zunger, Phys. Rev. B **77**, 241201 (2008).
[37]H. Monkhorst and J. Pack, Phys. Rev. B **13**, 5188 (1976).
[38]F. Murnaghan, Proc. Natl. Acad. Sci. (USA) **30**, 244 (1944).
[39]M. P. Molepo and D. P. Joubert, Phys. Rev. B **84**, 094110 (2011).
[40]A. V. Krukau, O. A. Vydrov, A. F. Izmaylov, and G. E. Scuseria, J. Chem. Phys. **125**, 224106 (2006).
[41]O. Madelung, *Semiconductors: Data Handbook* (Springer, Berlin, 2003).
[42]W. Roth, Phys. Rev. **110**, 1333 (1958).
[43]A. K. Cheetham and D. A. O. Hope, Phys. Rev. B **27**, 6964 (1983).
[44]K. Marklund and S. Mahmoud, Phys. Scr. **3**, 75 (1971).
[45]S. Desgreniers, Phys. Rev. B **58**, 14102 (1998).
[46]S. Adachi, *Optical Properties of Crystalline and Amorphous Semiconductors: Numerical Data and Graphical Information* (Kluwer Academic, Dordrecht, 1999).
[47]J. Zhang, Phys. Chem. Miner. **26**, 644 (1999).
[48]F. S. Saoud, J. Plenet, L. Louail, and D. Maouche, Comput. Theor. Chem. **964**, 65 (2011).
[49]S.-H. Wei and A. Zunger, Phys. Rev. B **48**, 6111 (1993).